Numerical study of fatigue cracks propagation in a high strength steel

Tiago Santos

tiagosantos91@hotmail.com

Instituto Superior Técnico, Universidade de Lisboa

December 2017

Abstract

The study and evaluation of the mechanical and structural components integrity is an extremely important task in engineering. Fracture Mechanics is the field of mechanics concerned with the study of fracture strength in materials, which can be used to study the fatigue in materials. One parameter which allows quantifying the fracture strength is the Stress Intensity Factor, K.

In the present work the fatigue strength in 3 different configurations of specimens (Compact Tension) of a high strength steel is evaluated, two of them having welding configurations (longitudinal and transversal weld), in order to determine the geometry effects on the fatigue crack growth. To evaluate those effects a numerical study in the finite element commercial software Abaqus® is performed for each specimen. Firstly, the stress intensity factor, K is calculated in a static analysis using the extend finite element method (XFEM) comparing the values with the theoretical ones, in which is obtained an average difference of 7%, for the non-welded specimen. The welding geometries, have a slightly lower K value, with a range from 1 to 2% in the longitudinal welded specimen. From 5 to 9% in the transversal welded specimen, where the crack intersects the weld.

The numerical study of fatigue propagation crack, is made in Abaqus® using the XFEM for a cyclic analysis, where the crack propagates according with the Paris' Law, with an average error of 2% comparative with the theoretical values from the non-welded specimen. In the welded specimens an increase in the fatigue strength in the specimen where the crack intersects the weld is verified, lowering the value of K, because the weld material is the same as the weld and also the heat affected zone is not considered. Actually, the heat affected zone increases the value of K. The propagation crack growth in the transversal welded specimen is reduced for almost half the cycle, when the crack intersects the weld.

Keywords: Fracture Mechanics, fatigue propagation cracks, stress intensity factor, XFEM, Abaqus®

1. Introduction

Failure by fatigue crack growth is a potential problem for component/structures that are subject to cyclic loadings, compromising reliability and safety. Due to these facts, specimens are made to test the fatigue strength of the materials under specific machines. This type of tests requires effort, money and time. One solution is to perform finite element analysis (FEA) in order to verify the experimental data and make more complex geometries. The commercial Abaqus® software simulates the crack and the respective propagation, using the eXtended Finite Element Method (XFEM) [1], [2] which is an independent mesh method. This method allows the stress intensity factor (SIF) calculation for a stationary crack. Also using the XFEM the Paris' Law [3] can be used to simulate the crack propagation combined with the low cycle fatigue (LCF) analysis.

In order to evaluate the fatigue strength and study the fatigue crack growth a numerical study using the software Abaqus® is performed in a high steel strength specimen, more precisely a compact tension (CT). The specimen have a specific geometry following specific standards like the ones proposed by the American Society for Testing Materials (ASTM), E 399/ E 647 [4], [5], providing the analytic solution to calculate the SIF for different crack lengths and nominal applied load.

2. Fracture Mechanics applied to fatigue crack propagation

Firstly, there are two approaches in the fracture mechanics: Linear Elastic Fracture Mechanics (LEFM) and the Elastic-Plastic Fracture

Mechanics (EPFM). The one studied in the present work is the LEFM. The LEFM only considers a small plastic zone around the crack tip and the remaining zone with an elastic linear behaviour. The zone where the crack tip is located, is a zone with a high concentration of tensions. There are 3 loading modes (fig. 1) which originate a crack and respectively propagation.

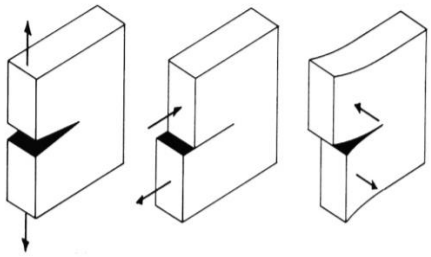

Figure 1 – Loading modes: (a) mode I (b) mode II (c) mode III [6]

The mode I is the one studied in this work, due to being the most common and the more critical, where the tensile stress is normal to the crack plane. To characterize the crack tip the stress intensity factor is a parameter useful to provide a fracture criterion for the material. The stress intensity factor for mode I can be expressed by the general form:

$$K_I = Y\sigma\sqrt{\pi a} \tag{1}$$

Where, Y is the geometric factor dependent on the geometry and the applied load, σ is the normal tension and a is the crack length.

The compact tension specimen (fig. 2) evaluated in this work in accordance with the standard E 399/E 647 [4], [5] is written in the following form:

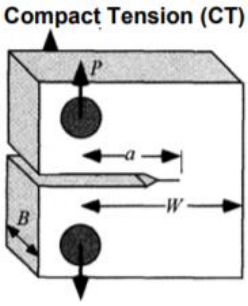

Figure 2 - Compact Tension Specimen [6]

$$K_I = \frac{P}{B\sqrt{W}} f\left(\frac{a}{W}\right) \tag{2}$$

Where, $f\left(\frac{a}{W}\right)$ is:

$$\frac{2+\frac{a}{W}}{\left(1-\frac{a}{W}\right)^{\frac{3}{2}}}\left[0.886 + 4.64\left(\frac{a}{w}\right) - 13.32\left(\frac{a}{w}\right)^2 + 14.72\left(\frac{a}{w}\right)^3 - 5.6\left(\frac{a}{w}\right)^4\right]$$

Another parameter used to characterize the crack tip is the energy release rate, given by the letter G, which was proposed by Irwin [7] based on the work of Griffith [8] who discovered when the crack propagates it releases energy that can be quantified. The K_I relates with the G in the following way:

$$G = \frac{{K_I}^2}{E'} \tag{3}$$

Where $E' = E$ for plane stress and $E' = \frac{E}{1-\nu^2}$ for plane strain, E is Young's Module and ν is Poisson's coefficient. In this work, the plane stress convention is considered.

Paris' Law [3] is used for the fatigue crack propagation in materials with a linear elastic behaviour like the one studied in the present work. Paris' Law can be described as (fig. 3):

$$\frac{da}{dN} = C\Delta K^m \tag{4}$$

Where C and m are material constants obtained experimentally and ΔK the variation of SIF under a cyclic loading.

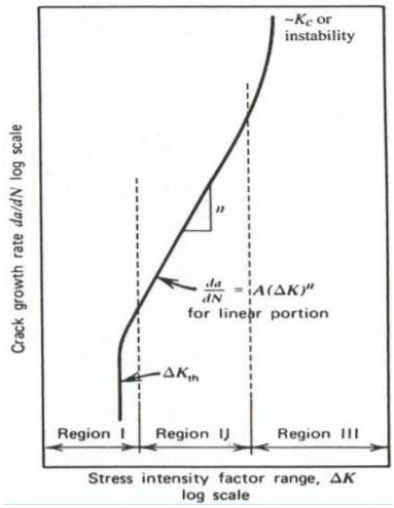

Figure 3 - Log-log plot of da/dN versus ΔK [6]

Paris' Law can be applied for the region II of the curve, where the crack propagates under a stable evolution. In the region I the fatigue crack has a slow propagation and in the region III the crack evolution is unstable.

To calculate the number of cycles the eq. 4, can be integrated obtaining the following equation:

$$N = \int_{a_i}^{a_f} \frac{da}{C\Delta K^m} \tag{5}$$

Where N is the number of cycles for a correspondent crack length a. Note that this type of study is made with a constant amplitude of cyclic loading.

3. Finite Element Method

The finite element analysis states that a major problem is subdivided into smaller problems [9]. These types of methods for numerical studies are very common in engineering dealing with problems such as structural analysis, heat transfer and fluid flow. The problems are divided in smaller problems with a finite number of variables called elements with well-defined properties.

The combination of elements in a geometry is called a mesh. For example, in 3D geometry a mesh with hexahedron elements is applied where the vertices of the elements are called nodes. Under a load application, the nodes move from one position to another passing from an un-deformed shape to a deformed shape. That deformation simulates the reality and the displacements on the nodes allows to calculate the tensions in the geometry.

eXtended Finite Element Method

The XFEM was developed in 1999 by Belytschko and Black [1] in order to overcome the limitations on the basic Finite Element Method (FEM) on discontinuities like cracks.

The XFEM uses enrichment functions. Those functions typically consist of near-tip asymptotic functions that capture the singularity around the crack tip and a discontinuous function that represents the jump in the displacement across the crack surfaces. The approximation for a displacement vector function with the partition of unity enrichment is [9]:

$$u^h = \sum_{i=1} N_i(x) \left[u_i + H(x) a_i + \sum_{\alpha=1}^{4} F_\alpha(x) b_l^\alpha \right] \quad (6)$$

Where $N_i(x)$ are the usual nodal shape functions; u_i is the usual nodal displacement vector associated with the continuous part of the finite element solution; the second term is the product of the nodal enriched degree of freedom vector, a_i and the associated discontinuous jump function *Heaviside* $H(x)$ across the crack surfaces; and the third term is the product of the nodal enriched degree of freedom vector, b_l^α and the associated elastic asymptotic crack-tip functions, $F_\alpha(x)$. The first term on the right-hand side is applicable to all the nodes in the model; the second term is valid for nodes whose shape function support is cut by the crack interior; and the third term is used only for nodes whose shape function support is cut by the crack tip [1], [9]. The fig. 4, illustrates the enrichment functions.

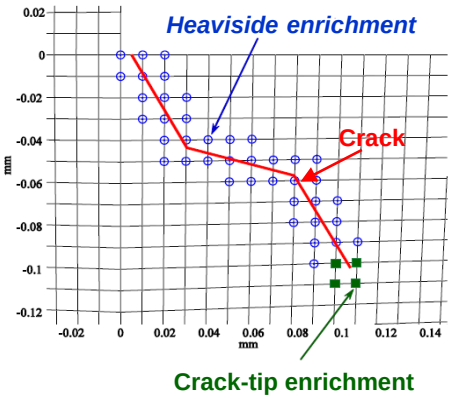

Figure 4 - Crack with the respectively enrichment functions [9]

As can be seen in the fig. 4, the XFEM is a meshless method, that does not require a specific mesh for the crack to propagate, which means a more precise evaluation in the fatigue propagation and SIF calculations.

4. Case study

In order to study the fracture mechanics, three CT specimens (fig. 5) are modelled in Abaqus®.

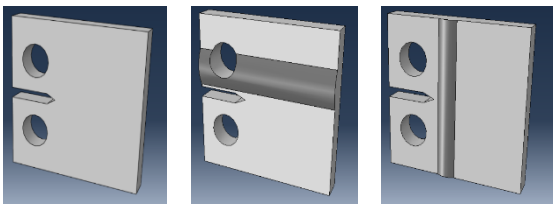

Figure 5 -Modelling (a) non-welded, (b) longitudinal welding, (c) transversal welding

The first one, is the standard CT specimen which can be compared with the analytical values from the literature; the second has a weld in the longitudinal direction with a weld thickness of 2 mm and 14 mm weld width; the third has a weld in the transversal direction with a weld thickness of 1 mm and 8 mm weld width. The thickness of all specimens is 8 mm and a useful width of 50 mm (distance from the centre holes to the end of specimen).

The CT specimen is pin-loaded by special clevises that applies forces in opposite direction in order to open the specimen (fig. 6). The crack will begin at the top of the notch and extend through the sample, this also being this the procedure simulated in Abaqus®.

There are two different tasks:

- Obtaining the SIF for different crack lengths in all specimens in a static analysis;
- Simulating the fatigue crack growth using the Paris' Law for all specimens in a cyclic analysis.

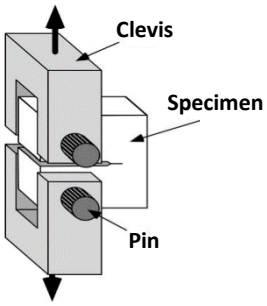

Figure 6 - Apparatus for testing compact specimens [6]

5. Numerical analysis

The numerical analysis is done in Abaqus® version 6.14-1. Firstly, the three specimens are modelled.

The crack surface is also modelled as a planar object, and introduced in the specimen at the top of the notch (fig. 7).

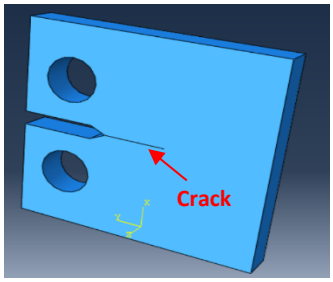

Figure 7 - Specimen with a crack

For the static analysis, the crack length is manually defined in a range between 11 mm to 40 mm, to obtain the correspondent SIF value. In the cyclic analysis the initial crack length is 11 mm and it propagates in accordance with the cycle number.

The material proprieties can be consulted in the table 1:

Young's Module [GPa]	Poisson's coefficient	C	m
200	0.3	$7.924e^{-10}$	2.7

Table 1 - Material properties

The constants C and m, are in the S.I. units **MPa**$\sqrt{m}$. The welding material is considered the same as the non-welded and heat affect zone (HAZ) is not considered, which result from the welding process modifying the material properties. The only change the weld affects in this study is the geometry.

The two pins are modelled as reference points in the centre of specimen holes, in the middle of specimen thickness, to guarantee that the load and the constraints are exactly applied in the middle. The reference points are coupled with the inner hole surfaces.

There are two loading cases in this work, a static load and cyclic load. Both have the nominal load of 10 000 N and are applied in one reference point (simulated pin). For the static analysis there is an initial state with no force applied and a final state with the applied force opening the crack for the pre-defined crack length. The fatigue cycle, the load is applied with an amplitude, shown in fig. 8.

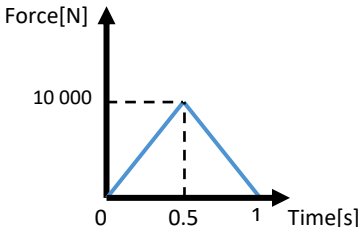

Figure 8 - Cyclic loading

The constraining conditions are applied to the other reference point, where the translations in x, y and z are fixed and the rotation in x and y also fixed.

Mesh

The mesh has a strong impact in the results. Factors like element density, distribution and the type of elements are crucial to obtaining valid results.

The elements type are the Continuum 3D 8-node Reduced integration (C3D8R), which are hexahedrons with 8 nodes.

Family	Library	Order	Type	Name

3D Stress	Standard	Linear	Hexahedron	C3D8R

Table 2 - Element properties

As already stated, in this work the plane stress convention is considered, as can be seen by the element family in table 2.

For the static analysis there are some techniques to obtain more precise values of K_I. One technique is the refinement at the crack tip [10], and increase the number of elements in the thickness direction.

Figure 9 - Refinement region at the crack tip

A quadrangular shape is drawn in the specimen (fig. 9), so that a specific number of elements can be defined at that zone.

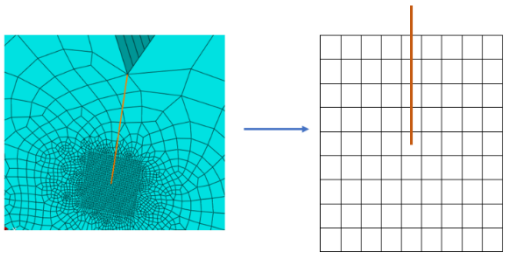

Figure 10 - Crack tip with elements respectively

The number of elements in the refinement zone has to be an odd number to guarantee the crack tip is perfectly centred (fig. 10) [10] .

For the cyclic analysis, where the fatigue crack growth is studied, a small chamfer with 1 mm length is made, to guarantee a path for the fatigue crack to follow, as shown in fig. 11.

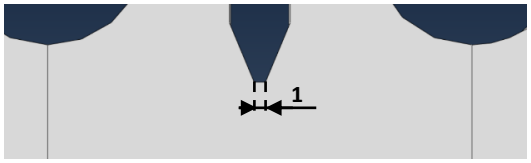

Figure 11 - Top notch replaced with a small 1 mm chamfer

This chamfer allows the section of a path with a well-defined length and width (fig. 12).

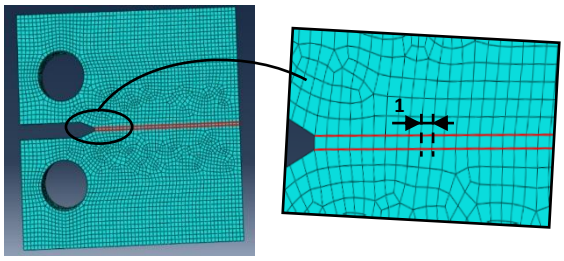

Figure 12 - Section path for the fatigue crack growth

The number of elements along the path is 1 mm, to guarantee that, when it grows, the crack is 1 mm at a time for a determined cycle number.

Elements number

For the static analysis a global mesh of 1.5 mm is chosen, and a study to converge the results at the crack tip and thickness element number is made. Table 3, contains the values for different cases in order to choose the best possible solution.

CASE	THICKNESS [ELEMENTS]	CRACK-TIP	TIME [SECS]	KIC [MPA.M$^{1/2}$]
1	5	5*5 (25)	15	57.47
2	10	5*5 (25)	23	57.39
3	15	5*5 (25)	33	57.21
4	15	11*11 (121)	43	57.27
5	15	15*15 (225)	53	57.15
6	15	21*21 (441)	55	57.15
7	25	21*21 (441)	99	57.16
8	15	35*35 (1225)	105	57.15

Table 3 - Convergence study with a machine Intel® Core™ i7-7700HQ CPU @ 2.80 GHz, 16 GB RAM

After case 5 the values tend to stabilize (fig. 13).

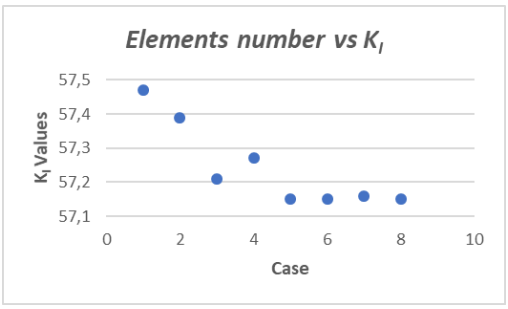

Figure 13 - Convergence graph

The mesh for case 6 was chosen with 15 elements in the thickness and a quadrangular zone with 21x21 elements. The total number of elements is shown in table 4:

Non-welded	Longitudinal welding	Transversal welding
57 225	62 445	47 625

Table 4 - Total number of elements, static analysis

For the cyclic analysis, the mesh has a global size of 1 mm, and the thickness has 8 elements, the total number is shown in table 5:

Non-welded	Longitudinal welding	Transversal welding
28 776	30 344	28 960

Table 5 - Total number of elements, cyclic analysis

6. Static analysis results

On Abaqus® a static analysis was performed, with the SIF output. The software gives the results for the three modes (K_I, K_{II}, K_{III}), but only mode I is studied. The results evolve along the material thickness (fig. 14).

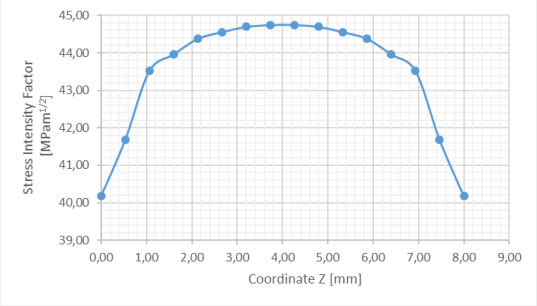

Figure 14 - Crack tip, for a crack length of 20 mm (Non-welded specimen)

The crack tip is symmetrical as the prediction in the literature on the crack tip, the maximum K_I is in half the thickness. The stress intensity factor varies with the crack length, as can be seen on fig. 15. The SIF value increases on a higher rate from a crack length 30 to 40 mm than a 15 to 30 mm, due to the high speed propagation as the crack length increases.

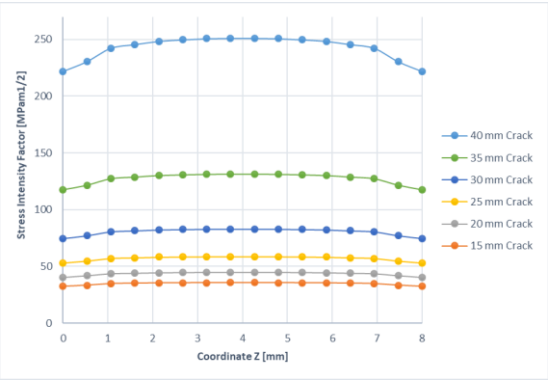

Figure 15 - SIF values for different crack length values

The high-tension concentrations can be seen on fig. 16.

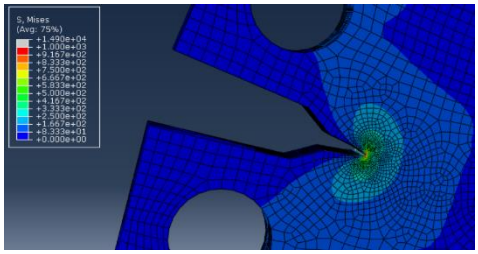

Figure 16 - Tension distribution around the crack-tip

For the results validation, the numerical solution is compared with the analytical one for the non-welded specimen in accordance with the standard E 399/E 647 [4], [5], which gives the eq. (2) already enunciated. Fig. 17, illustrates the difference between the two approaches and fig. 18, the error between them.

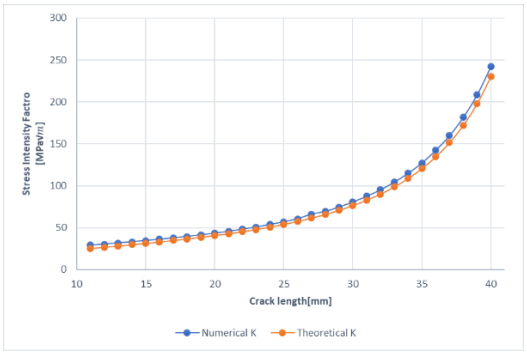

Figure 17 - Theoretical vs numerical curve

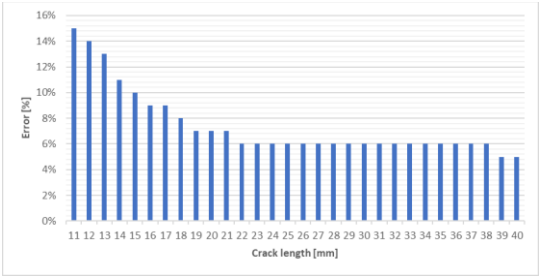

Figure 18 - Error between theoretical and numerical

The XFEM, proves to be a precise method to estimate the SIF, with an average 7% error from the literature.

After the results validation, the same study is performed for the two different specimens with welded configurations, to understand the effect of different geometries in the SIF value. The fig. 19, shows a comparison between the three different crack tips for a 15 mm crack tip, and the fig. 20, for a 25 mm crack tip.

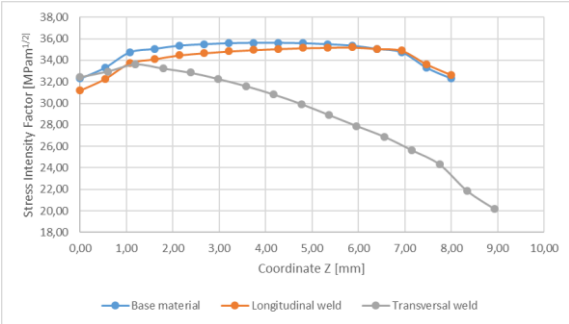

Figure 19 - Comparison for a 15 mm crack length

The 15 mm crack length has a lower value on the transversal weld because the crack tip is on the welded zone and the increase in the thickness specimen lowers the SIF value, the longitudinal and base are quite the same due to the fact the crack tip does not intersect the welded zone.

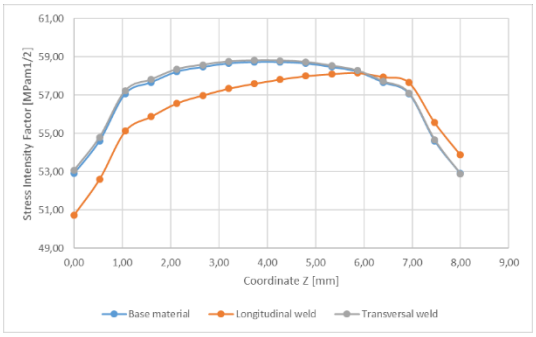

Figure 20 - Comparison for a 25 mm crack length

In the 25 mm crack length, the transversal weld and the non-welded are the same because the welded zone is already crossed and does not interfere with the SIF value. The crack tip in the longitudinal weld have a different geometry but the average SIF value is the same.

Fig. 21, illustrates the curves with the SIF values vs crack length for the three specimens, and the fig. 22, the differences between the two welded configurations with the non-welded.

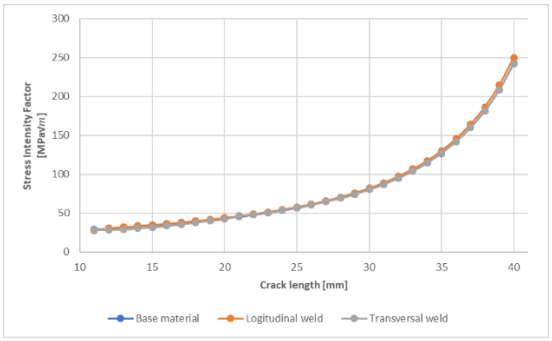

Figure 21 - SIF Comparison between the three specimens for different crack length

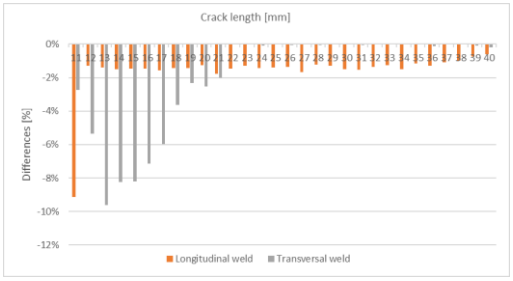

Figure 22 - Differences between the welded specimens with the non-welded

The differences are visible when the crack reaches the weld, having a lower SIF value. The crack in the transversal welded specimen from 13 to 21 mm is lower because the weld increases the thickness, reaching a difference of about 9%. In the longitudinal weld the difference is in range of 1 to 2% for all the crack lengths. The comparison is made with the numerical values from the non-welded.

7. Cyclic analysis results

The fatigue crack growth is simulated in Abaqus® accordingly with Paris' Law [3], but in Abaqus® the form is expressed in the form of energy release rate (fig. 23) and not the stress intensity factor [9], as shown on the eq. (7):

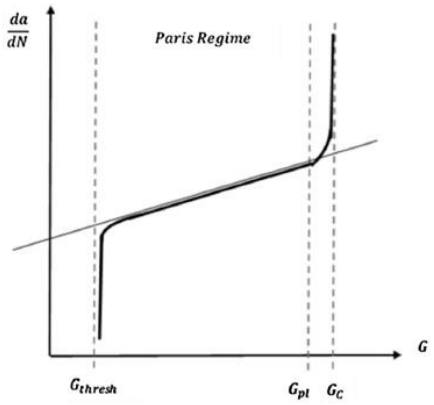

Figure 23 - Log-log plot of da/dN vs G

$$\frac{da}{dN} = c_3 \Delta G^{c_4} \qquad (7)$$

Where c_3 and c_4 are material constants, obtained by:

$$c_4 = \frac{m}{2} \qquad (8)$$

$$c_3 = C(E')^{c_4} \qquad (9)$$

The stress intensity factor can be related with the energy release rate as shown in eq. (3) before.

The results for the non-welded are validated with the integration of Paris' Law (eq. 5) using the integration based on Simpson method [11]. The fig. 24, shows the plot between the crack length and cycle numbers for both numerical and theoretical methods.

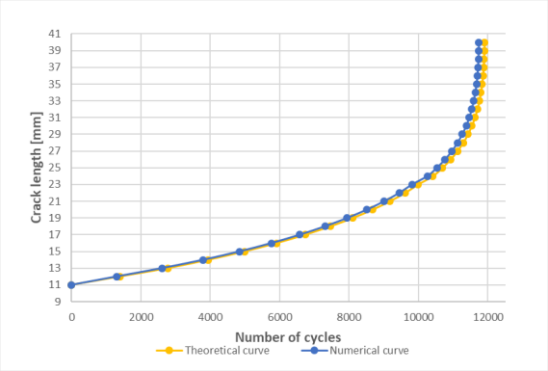

Figure 24 - Comparison between theoretical and numerical curve

As can be seen the results are very close to the theoretical ones with an average error of 2%. The fatigue crack propagates at a normal speed to around 10 000 cycles and then the propagation increases due to a decrease in the fatigue strength of the material. The same simulation is made for the two welded configurations to determine the effects of welded geometries in crack propagation.

Fig. 25 and 26, show a 20 mm fatigue crack in the longitudinal weld specimen and transversal weld specimen respectively.

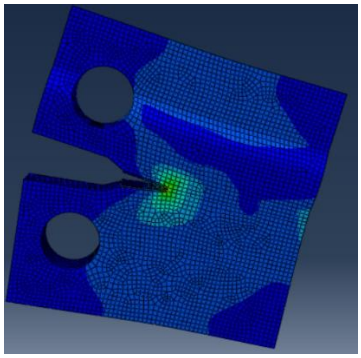

Figure 25 - 20 mm Fatigue crack in the longitudinal weld

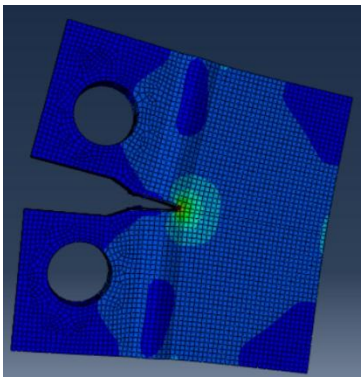

Figure 26 - 20 mm Fatigue crack in the transversal weld

Stress distribution in the longitudinal weld is affected by the weld as can be seen in fig. 25, in the superior part of the crack. But the crack does not go through the weld as in the transversal weld. In the transversal weld the stress distribution is symmetrical at the crack tip, as seen in the fig. 26. Table 6, shows the results for the three specimens.

	Number of cycles		
Crack length [mm]	Non-welded	Longitudinal weld	Transversal weld
11	0	0	0
12	1294	1246	1439
13	2603	2577	3079
14	3794	3807	5061
15	4838	4909	7470
16	5761	5900	9775
17	6579	6780	11700
18	7304	7560	13279
19	7946	8258	14403
20	8514	8881	15175
21	9013	9431	15679
22	9447	9916	16077
23	9815	10342	16460
24	10252	10715	16808
25	10529	11037	17109
26	10764	11314	17366
27	10962	11551	17584
28	11127	11756	17768
29	11263	11925	17921
30	11375	12067	18048
31	11465	12185	18153
32	11537	12281	18238
33	11594	12359	18306
34	11638	12422	18360
35	11671	12471	18402
36	11696	12509	18435
37	11714	12538	18460
38	11727	12561	18479
39	11736	12577	18492
40	11742	12588	18499

Table 6 - Numerical results, Number of cycles vs crack length

As seen in the table 6, the initial crack length of 11 mm appears as 0 cycles because in this work only crack propagation is studied not the initiation, so a pre-crack of 11 mm is introduced in the specimens.

The results show that both longitudinal and transversal weld have higher fatigue strength, in the longitudinal weld the difference is an average 5% more compared to the non-welded. This minimal difference is due to the fact that the fatigue crack does not intersect the welded zone, so the effects are not so as obvious as expected.

In the transversal weld specimen on the 13 mm crack length, the fatigue crack intersects the welded zone and an increase in the number of cycles from there forward is noticeable, reaching a maximum difference about 82% compared to the non-welded propagating more slowly than the non-welded, and consequently an increase in the fatigue strength. After 21 mm of crack length, the fatigue crack leaves the welded zone and the propagation is made at a normal speed. Fig. 27, shows the three-different crack lengths vs number of cycles.

The crack slows the propagation when it intersects the weld in the transversal welded specimen as can be seen in the fig. 28.

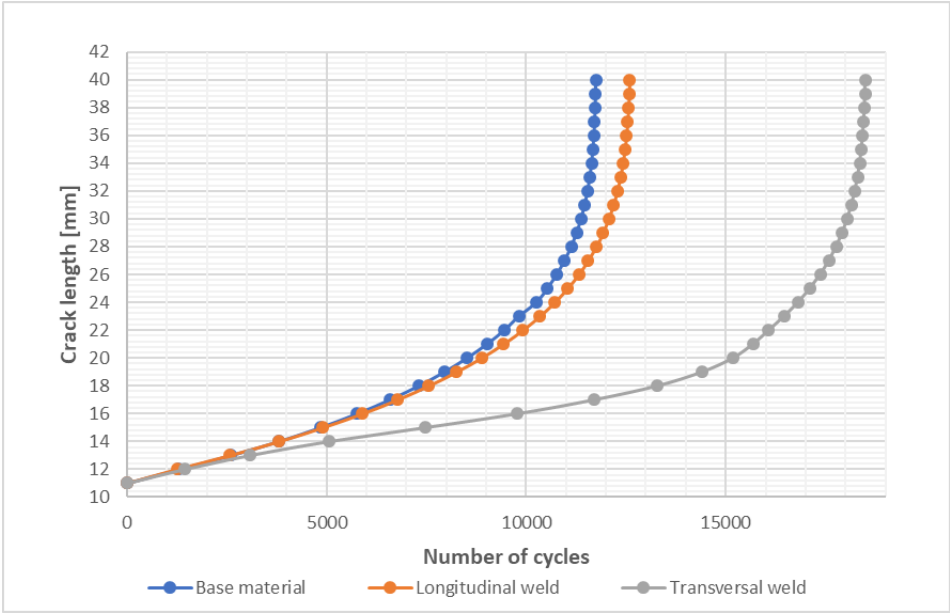

Figure 27 - Crack length vs number of cycles for the three specimens

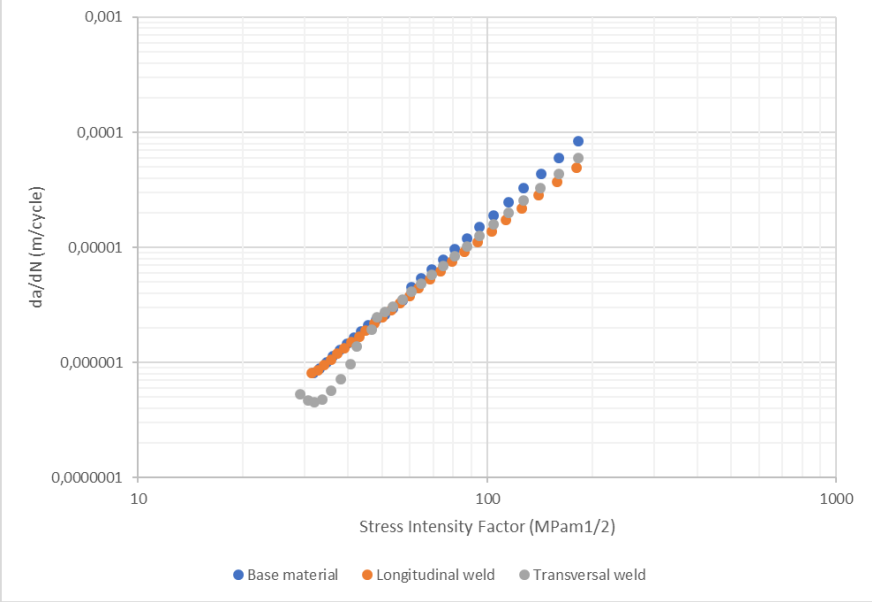

Figure 28 - da/dN vs ΔK for the three specimens

8. Conclusions

The main conclusions are

- According to the SIF numerical results, XFEM values are closer to the theoretical values and approximately 7% higher than the theoretical values. Thus, very good correspondence exists between SIFs obtained using XFEM and theoretical results confirming the robustness and accuracy of the developed XFEM formulation;
- The welded configurations have lower SIF values, due to the increase in thickness, being more noticeable when the crack intersects the weld as in the case of the transversal weld;
- The crack propagation using the XFEM presents good results comparing to the theoretical values with an average difference of 2%, the numerical results being lower than the theoretical values, presenting a more conservative method;
- The fatigue crack growth is highly affected when it intersects the weld zone, due to an increase in specimen thickness. The longitudinal weld is never reached by the crack, so the average difference comparing with the non-welded is 5% lower. The transversal one reaches an 82% lower propagation in maximum thickness on the welded zone.

Leading to the conclusion, that the welded specimens have a higher fatigue strength.

Acknowledgments

This work was supported by FCT, through IDMEC, under LAETA

References

[1] T. Belytschko and T. Black, “Elastic crack growth in finite elements with minimal remeshing,” *Int. J. Numer. Methods Eng.*, vol. 45, no. 5, pp. 601–620, 1999.

[2] D. S. Simulia, “Mesh-independent Fracture Modeling (XFEM),” *Modeling Fracture and Failure*.

[3] P. Paris and F. Erdogan, “A critical analysis of crack propagation laws,” *J. Basic Eng.*, vol. 85, no. 4, pp. 528–533, 1963.

[4] ASTM E 399-90, “Standard Test Method for Plane-Strain Fracture Toughness of Metallic Materials,” vol. 90, no. Reapproved, pp. 1–31, 2012.

[5] ASTM E 647-00, “Standard Test Method for Measurement of Fatigue Crack Growth Rates,” *ASTM Int.*, vol. 3, pp. 1–43, 2001.

[6] T. L. Anderson, *Fracture Mechanics: Fundamentals and Applications*, 3ª. CRC Press, 2005.

[7] G. R. Irwin, “Analysis of Stresses and Strains Near the End of a Crack Traversing a Plate,” *Journal of Applied Mechanics*, vol. 24, no. September. pp. 361–364, 1957.

[8] A. A. Griffith, “The Phenomena of Rupture and Flow in Solids,” *Philos. Trans. R. Soc. A Math. Phys. Eng. Sci.*, vol. 221, no. 582–593, pp. 163–198, 1921.

[9] D. S. Simulia, “Abaqus 6.14 Online Documentation,” 2014.

[10] M. Levén and R. Daniel, “Stationary 3D crack analysis with Abaqus XFEM for integrity assessment of subsea equipment,” 2012.

[11] K. E. Atkinson, *An Introduction to Numerical Analysis*, vol. 125, no. 1–2. 1989.